Eur Biophys J (1997) 26: 371–380

ARTICLE

L. Schreiber · K. Schorn · T. Heimburg

^{2}H NMR study of cuticular wax isolated from *Hordeum vulgare* L. leaves: identification of amorphous and crystalline wax phases

Received: 1 February 1997 / Accepted: 27 May 1997

Abstract ^{2}H-NMR spectra of perdeuterated octadecanoic acid (C_{18}AC) and dotriacontane (C_{32}AN) added to isolated and subsequently recrystallized cuticular wax from barley (*Hordeum vulgare* L.) leaves were recorded between 298 and 328 K. They were compared to calorimetric excess heat capacity profiles. The NMR-data revealed the presence of both an isotropic and a rigid wax component at temperatures below 313 K. At temperatures above 318 K all labels are in the fast motion regime indicating a transition in the host matrix of the labels. The presence of the surfactant C_6E_3 reduced the order of the C_{18}AC-label but did not influence the order of the long chain alkane label (C_{32}AN). Most surprisingly, calorimetry revealed that most thermotropic events take place above the apparent melting observed in NMR. Furthermore, the macroscopic softening and melting of the wax took place in the same temperature regime as in the calorimetric experiments. The excess heat capacity traces were complex and indicated a heterogeneous structural composition of the barley wax. We interpreted the apparent conflict between the NMR and the calorimetric results by assuming a crystalline host matrix, formed by C_{26}-alcohol, the major molecular component of the wax. Within the crystal compartments there may exist an amorphous matrix with some crystalline microdomains of other wax components, including the NMR-labels. The melting of the amorphous environment leads to fast motional narrowing of the NMR spectral line of the microdomains without melting of the macroscopic structure. The measurements of diffusion coefficients (D) of radiolabelled C_{18}AC and C_{32}AN gave additional insight into the microstructure of the way architecture. Identical results in terms of D were obtained when radiolabelled C_{18}AC was added to the wax from either the exterior after recrystallization or when it was recrystallized together with the wax. It is concluded that in both cases the radiolabelled molecule is located in an amorphous wax phase, which forms a percolating path through the wax and is thus also accessible to the surfactant C_6E_3. In contrast, D of C_{32}AN in barley wax was about 2400 times higher when C_{32}AN was added to recrystallized wax from the exterior compared to wax samples recrystallized together with C_{32}AN. This indicates that in the case of C_{32}AN the alkane is trapped within separate microdomains of the wax during recrystallization and thus it remains essentially immobile, whereas it possesses a high degree of mobility when it is added from the exterior where it has only access to the percolating amorphous wax phase.

Key words Crystallinity · Cuticular wax · Deuterium NMR · Diffusion coefficient · Plant cuticle · Percolation

L. Schreiber (✉)
Julius-von-Sachs-Institut für Biowissenschaften,
Lehrstuhl für Botanik II, Universität Würzburg,
Mittlerer Dallenbergweg 64, D-97082 Würzburg, Germany
(Fax: +49-931-888-6235; e-mail: lukas@botanik.uni-wuerzburg.de)

K. Schorn · T. Heimburg
Max-Planck-Institut für Biophysikalische Chemie,
Abteilung Spektroskopie,
Am Fassberg, D-37077 Göttingen, Germany

1 Introduction

The plant cuticle is an extracellular polymer covering the above-ground organs, mainly the leaves, of all higher plants (Martin and Juniper 1970; Cutler et al. 1982) and thus forms the interface between the living plant interior and the atmosphere (Schönherr and Riederer 1989). The main function of the cuticle is the reduction of the evaporation of large amounts of water from the living parts of the plants into the atmosphere in order to protect the plant from desiccation (Schönherr 1982). Furthermore, the cuticle often forms an important barrier to the uptake of foliar pesticides, which have to penetrate the cuticle in order to develop their physiological action in the living plant cells (Bukovac 1976; Schönherr and Baur 1994). Chemically the cuticle is a heterogeneous, essentially lipophilic biopolymer consisting of esterified hydroxyfatty acids

(Kolattukudy 1980; Holloway 1982), the cutin matrix (MX), and soluble cuticular lipids (SCL) or waxes (Baker 1982; Walton 1990), which are deposited in the MX. The waxes, which form solid, partially crystalline aggregates at room temperature (Sitte and Rennier 1963; Reynhardt and Riederer 1991; Reynhardt and Riederer 1994), are essential for the transport barriers of the intact cuticular membranes since removal of the cuticular waxes increases cuticular permeability for water and organic molecules by factors in the range 10 to more than 1000 (Schönherr 1976; Riederer and Schönherr 1985).

For this reason it is important to obtain more data about cuticular waxes in order to understand their function as the transport barrier of the intact plant cuticle on a molecular level. Information is needed on: (i) wax composition, (ii) transport properties of waxes and (iii) the physical structure of waxes. In the past a number of independent studies have investigated the transport properties of cuticular waxes by diffusion experiments (Schreiber and Schönherr 1993; Schreiber 1995; Schreiber et al. 1996 a, b) and the physical structure of waxes by spectroscopic experiments (Basson and Reynhardt 1988; Reynhardt and Riederer 1991, 1994). On the basis of these results a model describing the architecture of the waxy transport barrier of the plant cuticle on a molecular level has been postulated (Riederer and Schreiber 1995). It was argued that the wax consists of an amorphous and a crystalline phase. Diffusion of penetrating compounds such as water or small organic molecules (e. g. pesticides) should be possible in the amorphous wax phase. Additionally, the simultaneous presence of highly ordered crystalline domains in the wax should form an excluded volume for the transport of penetrating molecules, thus increasing the path length of diffusion. However, direct evidence for this model is still missing.

Therefore, it was the purpose of this investigation to correlate results obtained by ^{2}H NMR spectroscopy with diffusion experiments of radiolabelled chemicals in the wax in order to investigate this postulated molecular transport model. We used ^{2}H-NMR as a tool to investigate the transition properties of the plant waxes and the influence of surfactants on the molecular structure. Solid state ^{2}H-NMR in the past has been extensively used to study dynamic properties of biological or artificial membranes (for reviews see: Seelig 1977; Seelig and Seelig 1980; Mantsch et al. 1977; Smith 1983). Owing to the chemical shift anisotropy, slow molecular motion results in characteristic, broad spectra which average to one single line upon fast isotropic molecular rotation. This effect can be used to study transitions which are linked to changes in molecular dynamics as in melting transitions of waxes or chain melting transitions of lipids. These investigations were supported by calorimetric measurements, recording the uptake of heat during a melting transition. The temperature dependence of the calorimetric profiles in heterogeneous samples is an important method for the construction of phase diagrams, which reveal the mixing properties of the wax components (Lee 1977; Heimburg et al. 1992).

2 Materials and methods

2.1 Plant materials

Barley plants (*Hordeum vulgare* L. cv. Magie) were cultivated in growth chambers (16 h light at 500 – 800 μmol m^{-2} s^{-1} PAR, 298 K and 50% R. H.; 288 K and 90% R. H. during the dark). Leaves from 4 to 6 week old plants were sampled and cuticular waxes were extracted with chloroform (3 s; 298 K) as described previously (Schreiber and Schönherr 1993). Extracts were filtered twice and the solvent volume was reduced to obtain a final wax concentration of about $5 \cdot 10^{-5}$ kg cm^{-3}. Until they were used in the experiments the wax solutions were stored at 248 K.

2.2 Chemicals

The monodisperse alcohol ethoxylate triethyleneglycol monohexylether (C_6E_3) (Fig. 1) was obtained from Fluka (Neu-Ulm, Germany). Chemical purity of 98% was checked by gas chromatography/mass spectrometry (Hewlett-Packard gas chromatograph 5890 series II equipped with a mass selective detector model 5971 A; Hewlett-Packard, Millville, NJ, USA). Perdeuterated octadecanoic acid (C_{18}AC) and dotriacontane (C_{32}AN) (Fig. 1) were obtained from IC Chemikalien (Ismaning, Germany). Both perdeuterated compounds had a chemical purity better than 98% as checked by gas chromatography/mass spectrometry. ^{14}C-labelled octadecanoic acid (specific radioactivity: 2 GBq $mmol^{-1}$) and dotriacontane (specific radioactivity: 0.38 GBq $mmol^{-1}$) were obtained from Amersham Buchler (Braunschweig, Germany) and Sigma (Deisenhofen, Germany), respectively. Radiochemical purity of ^{14}C-labelled compounds was better than 98% as checked by radio-TLC (TLC-Linear Analyzer, Tracemaster 20, Berthold, Wildbad, Germany).

2.3 ^{2}H NMR studies

Two wax samples were prepared by adding $2.5 \cdot 10^{-5}$ kg of the perdeuterated compounds (C_{18}AC or C_{32}AN) to $5 \cdot 10^{-4}$ kg barley wax dissolved in 10 cm^3 chloroform. Additionally, two further wax samples were prepared, which contained $0.5 \cdot 10^{-7}$ kg C_6E_3 besides the perdeuterated compound, in order to investigate the interaction of the alcohol ethoxylate with the barley wax. The ratio of $0.5 \cdot 10^{-7}$ kg C_6E_3 per $5 \cdot 10^{-5}$ kg wax was chosen for the experiments since it corresponds exactly to the maximum amount of C_6E_3, which is adsorbed into the wax in equilibrium with an external aqueous solution of C_6E_3 significantly above the critical micelle concentration (Schreiber et al. 1996 b). The solvent was evaporated for several days until a constant weight (Sartorius Microbalance, Göttingen, Germany; accuracy ±1.0 μg) of the residual wax sample was obtained. Finally, the dry wax samples were transferred into small glass tubes of 0.7 cm^3 volume

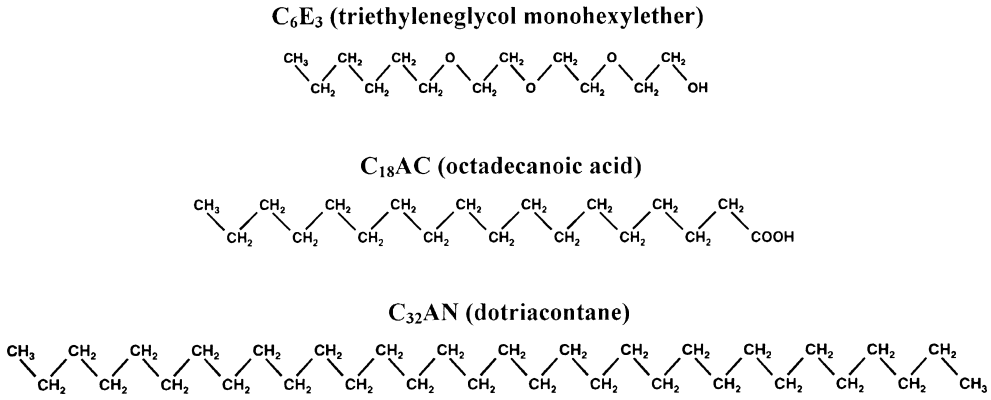

Fig. 1 Chemical structures of the 3 substances, C_6E_3 (triethyleneglycol monohexylether), $C_{18}AC$ (perdeuterated octadecanoic acid) and $C_{32}AN$ (perdeuterated dotriacontane) used in the ^{2}H-NMR experiments

($3.5 \cdot 10^{-2}$ m length; $5 \cdot 10^{-3}$ m inner diameter) and used for the ^{2}H NMR experiments. ^{2}H NMR spectra were recorded at a frequency of 46.1 MHz using a Bruker MSL-300 spectrometer (Bruker Analytische Meßtechnik GmbH, Rheinstetten, Germany). The quadrupole echo sequence with phase alternation was employed with 30 μs delays between 90° pulses of 6 μs and a recycle time of 1 s. Spectra were recorded at 298, 303, 308, 313, 318 and 328 K, thus covering a temperature range of 30 K. At each temperature several tens of thousands of scans were recorded and averaged. NMR spectra were normalized to constant area.

2.4 DSC experiments

Calorimetric experiments were performed on a differential scanning calorimeter from Calorimetric Sciences Corp., Provo, Utah. The calorimeter response time is about 90 s. A scan rate of 10°/h was used in the temperature range 273–373 K. Sample quantities were 10–20 mg. All heat capacity traces are given in units of J/g. The calorimetric experiments were checked for reproducibility and reversibility in successive up and down scans. Data were displayed after subtraction of a baseline, which was obtained from polynomial fitting of the C_p-trace outside of the range where the thermotropic events took place. Baselines obtained in this way were smooth and displayed no discontinuous features.

2.5 Diffusion experiments

Diffusion coefficients of ^{14}C-labelled $C_{18}AC$ and $C_{32}AN$ were determined by applying the desorption method previously described in detail by Schreiber and Schönherr (1993). In short, aluminium disks (1 cm^2 surface area) were immersed in chloroform solutions having a wax concentration of $5 \cdot 10^{-5}$ kg cm^{-3}. After evaporation of the solvent, aluminium disks were covered with a homogeneous layer of wax. In order to improve the adhesion of the wax to the surface of the aluminium disks, they were for 5 minutes heated to 373 K, which is above the melting point of the wax. The amount of wax covering the aluminium surface was determined by subtracting the weight of the aluminium disks from the final weight of the wax-covered aluminium disks using an electronic microbalance (Sartorius, Göttingen, Germany; accuracy: ±1 μg). The average thickness of the investigated wax layers was $1.5 \cdot 10^{-6}$ m ± $0.5 \cdot 10^{-6}$ m, using a wax density of $0.9 \cdot 10^3$ kg m^{-3} (Büscher 1960) for the calculation of the thickness.

Diffusion coefficients were determined after adding the ^{14}C-labelled compounds to the wax in two different ways. *Internal loading* of the wax refers to the addition of the ^{14}C-labelled compounds to the wax/chloroform solution prior to recrystallization. The wax was recrystallized together with the ^{14}C-labelled compound and subsequently the ^{14}C-labelled compound was desorbed again by immersing the wax samples into a phospholipid suspension (PLS; soy bean lecithin; Fluka, Neu-Ulm, Germany) as the desorption medium. Alternatively, recrystallized wax samples were loaded with the ^{14}C-labelled test compound from an external aqueous solution containing the radioactivity, which is referred to as *external loading*. $C_{18}AC$ was dissolved in citric acid (10 mol m^{-3}; pH 3.0), whereas $C_{32}AN$ was applied in a 10^{-3}% phospholipid suspension, in order to keep the lipophilic alkane solubilized in the external donor solution. Wax samples were immersed in these radioactive solutions for 48 hours, which guaranteed that a substantial amount the radioactivity was adsorbed in the wax. Subsequently, wax samples were removed from the radioactive solutions, blotted carefully on cellulose paper in order to remove radioactive donor solutions adhering to the surface of the samples and finally they were also desorbed with a 1% PLS solution.

Desorption experiments were carried out by incubating single wax samples, after internal or external loading, in 5 cm^3 glass vials containing the desorption medium (PLS). Vials were closed with screw caps and rotated (60 rpm) in the dark at 298 K. After defined periods of time the desorption media in each vial were replaced by fresh solutions and sampled radioactivity was measured by liquid scintillation counting (TRI Carb 2000, Canberra Packard, Frankfurt, Germany) after adding an adequate amount of scintillation cocktail (Ultima Gold XR, Canberra Packard, Frankfurt, Germany) to the samples. At the end of the de-

sorption experiment the amount of radioactivity remaining in the wax sample was also determined by immersing the wax sample in 200 µl chloroform in order to redissolve the wax together with the radioactivity from the aluminium. Subsequently the scintillation cocktail was added to the samples and they were counted as described above.

Desorption kinetics could be linearized for up to 50% desorption (Figs. 7 and 8), by plotting the relative amounts desorbed from the wax samples versus the square root of time. Diffusion coefficients of the two ^{14}C-labelled compounds could be calculated from the slopes of regression lines fitted to the linearized desorption kinetics by applying Eq. (1) (Felder and Huvard 1980):

$$\frac{M_t}{M_0} = \frac{4}{\Delta x} \cdot \sqrt{\frac{D}{\pi}} \cdot \sqrt{t} \qquad (1)$$

where M_t/M_0 is the relative amount desorbed, Δx [m] is the thickness of the wax layer, D [m^2 s^{-1}] is the diffusion coefficient and t [s] is the time. Rearranging the term $\left(\frac{4}{\Delta x}\right)\sqrt{\frac{D}{\pi}}$, which is proportional to the slope of the regression, line, finally allows the calculation of the diffusion coefficient D of the ^{14}C-labelled compound in the wax sample.

3 Results

3.1 ^{2}H-NMR experiments

Normalized ^{2}H-NMR spectra of mixtures of barley wax with two different perdeuterated labels, C_{18}AC (Fig. 2) and C_{32}AN (Fig. 4), were recorded in the absence and presence of the surfactant C_6E_3 (panels a and b, respectively). The two labels of different chain length were chosen in the expectation that they would mix differently with the different components of the heterogeneous wax. At temperatures below 313–318 K the most prominent feature of the ^{2}H-NMR-data is the presence of both a broad and an isotropic spectral component, indicating the presence of both fluid and rigid regions in the wax. The broad component is characterized by a maximum splitting of about 125 kHz. The spectral display was chosen to cut off the isotropic component in order to emphasise the broad, immobilised spectral contribution. In the temperature range around 313 K in the presence of C_{18}AC and 318 K in the presence of C_{32}AN, the shape of the broad spectral component is subject to motional narrowing, and disappears in a narrow temperature interval. Above 318 K all labelled molecules are in the fast motion regime.

To quantify the effect of temperature and the addition of surfactant, the second moments of the spectra,

$$\int (\omega - \omega_0)^2 f(\omega)\, d\omega / \int f(\omega)\, d\omega ,$$

were calculated and plotted versus temperature (Figs. 3 and 5). $f(\omega)$ represents the spectral line shape and ω_0 is the centre of gravity. Second moments have frequently been used as an order parameter to evaluate changes in molecular motion (Smith 1984). The quantitative and qualitative behaviour of the two different deuterium labels in the barley wax host matrix is different. First, the order parameter of the C_{18}AC-label (Fig. 3) is smaller than the order parameter of C_{32}AN (Fig. 5). Secondly, the addition of the surfactant C_6E_3 leads to a lowering of the molecular order parameter below the NMR-melting transition for the fatty acid label, whereas it does not affect the order of the alkane label. This indicates that the two labels monitor a different environment of the host matrix, in agreement with

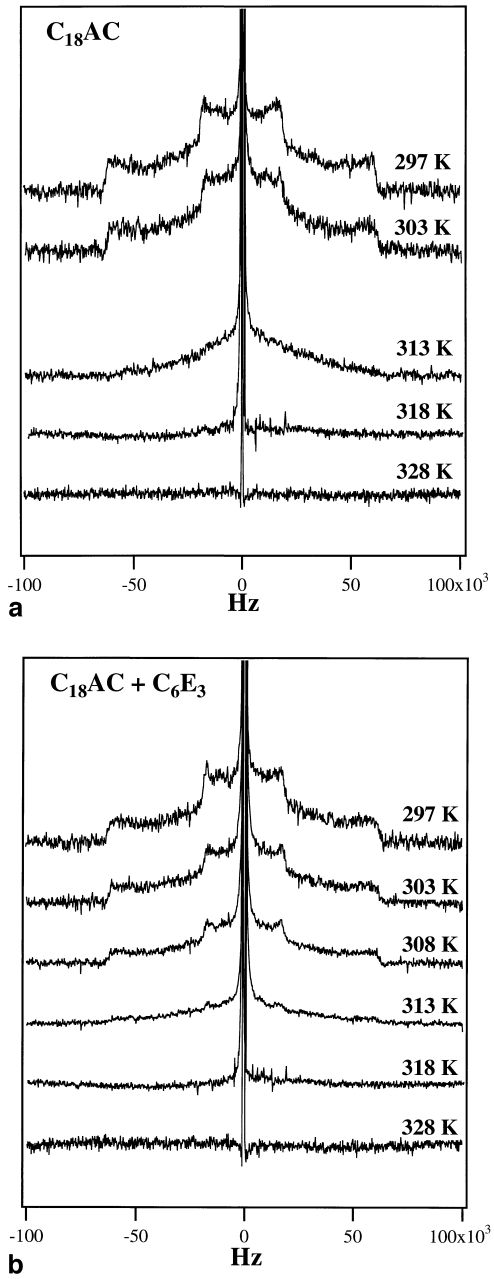

Fig. 2 **a** ^{2}H-NMR spectra of barley wax with 5% C_{18}AC perdeuterated label at different temperatures. Spectra were normalized to constant area. **b** Same sample as in **a** in the presence of 1% C_6E_3

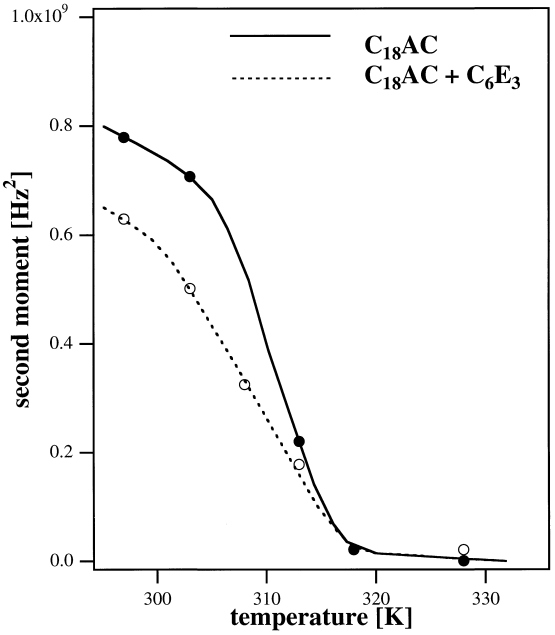

Fig. 3 Second moments of the spectra given in Figs. 2 a and b, indicating a reduction in molecular order upon addition of 1% of the surfactant C_6E_3 to barley wax samples labelled with $C_{18}AC$

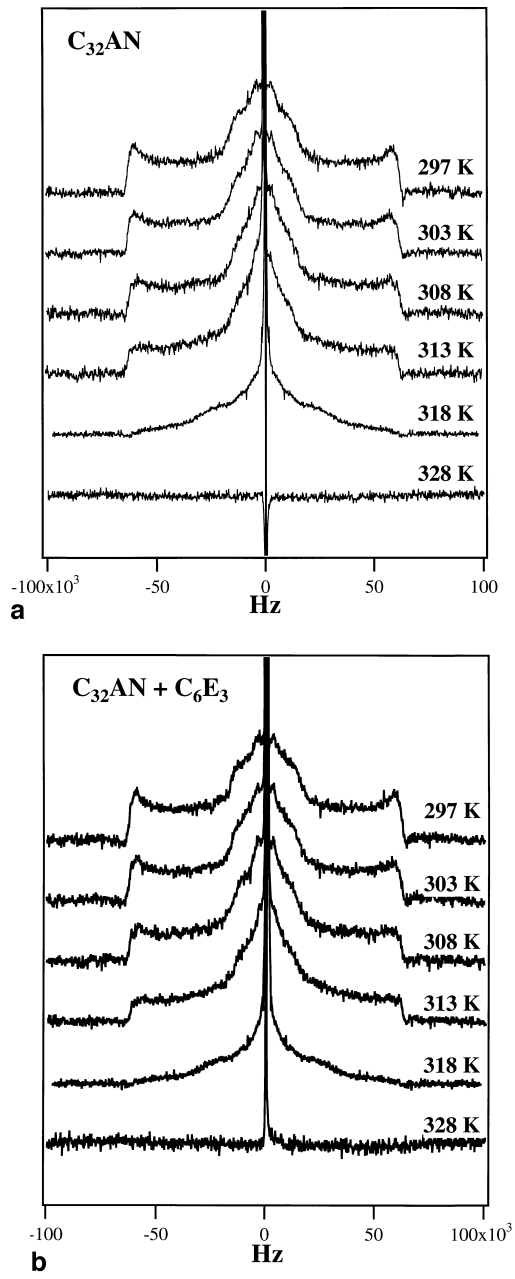

Fig. 4 **a** ^{2}H-NMR spectra of barley wax with 5% $C_{32}AN$ perdeuterated label at different temperatures. Spectra were normalized to constant area. **b** Same sample as in **a** in the presence of 1% C_6E_3

the calorimetric results, given below. On the other hand both labels display a rapid decrease in order at about 313–318 K, which suggests a significantly enhanced molecular motion above this temperature range, although the $C_{18}AC$ environment seems to melt at slightly lower temperatures than that of the $C_{32}AN$-label.

3.2 Calorimetric experiments

To further study the influence of the labels and the surfactant on the barley wax, we performed calorimetric experiments on the different mixtures, including the melting profiles of the pure components. This was done both to demonstrate miscibility of the NMR-labels with the barley wax and to correlate the wax melting with the ^{2}H-NMR data. Figure 6 a contains all traces related to experiments with $C_{18}AC$-labels. The bottom C_p-profile represents the pure perdeuterated label, indicating a melting point at 338.1 K. The top trace displays the melting of the barley wax with a more complex melting behaviour, reflecting the heterogeneous composition of the wax. It is apparent from the transition profile that the wax itself has a non-uniform structural composition and different components of the wax melt at different temperatures. Three heat capacity maxima can easily be recognised at 325.1, 339.7 and 347.1 K. The second peak corresponds roughly to the melting point of the label. The latter temperature corresponds to the melting point of the C_{26}-alcohol which constitutes about 80 weight% of the overall wax (Reynhardt and Riederer 1994). It should be noted that peaks in calorimetry do not necessarily correspond to the melting of defined components but may as well reflect temperature dependent changes in the composition of domains in different physical states. The two central curves reflect the barley wax labelled with 5% perdeuterated $C_{18}AC$ in the absence and in the presence of 1% C_6E_3, indicating four heat capacity maxima at 321.5, 330.9, 338.9 and 347.9 K. The surfactant itself has its melting point at about 265 K and is liquid in the temperature range given in Fig. 6 a, b.

Three important conclusions can be drawn: 1. The addition of the label changed the heat capacity profiles at temperatures different from the melting point of the pure

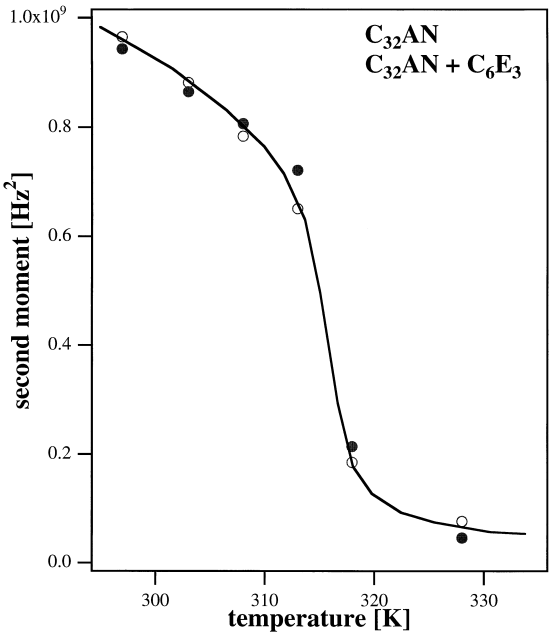

Fig. 5 Second moments of the spectra given in Fig. 4 a and b, indicating the absence of an effect on the molecular order upon addition of 1% of the surfactant C_6E_3 to barley wax samples labelled with $C_{32}AN$

label. No co-operative melting peak at the melting point of the pure label can be seen. From this it has to be concluded that the label mixes well with barley wax components. 2. The addition of surfactant has only a minor effect on the excess heat capacity. 3. Most surprisingly all calorimetric events take place above 318 K, which is apparently in conflict with the findings from ^{2}H-NMR or melting at about 313–318 K! We will attempt to explain this in the discussion section.

The corresponding experimental results of the wax in the presence of 5% perdeuterated $C_{32}AN$-alkane label are given in Fig. 6 b. The pure label has two transitions close to each other at 335.3 K and 337.9 K. The label itself is more than 98% pure (checked by gas chromatography/mass spectrometry) indicating that this melting behaviour most likely is not due to impurities. Thus, the first transition is probably a solid-solid-transition whereas the second one reflects the solid-liquid melting transition. The melting transition temperature is therefore roughly the same as that of the fatty acid-label, despite the different chain length. This is due to the difference in head groups. The two central traces in Fig. 6 b reflect the melting in the presence of the alkane label. Again the label displays good mixing with the wax. However, the specific head changes in the presence of the $C_{32}AN$ are different from those in the presence of the other label, displaying C_p-maxima at 330.2, 333.9, 338.6 and 348.1 K. In contrast to the $C_{18}AC$-label the calorimetric events are moved somewhat towards higher temperatures. Therefore both labels seem to mix differently with the different components of the heterogeneous wax.

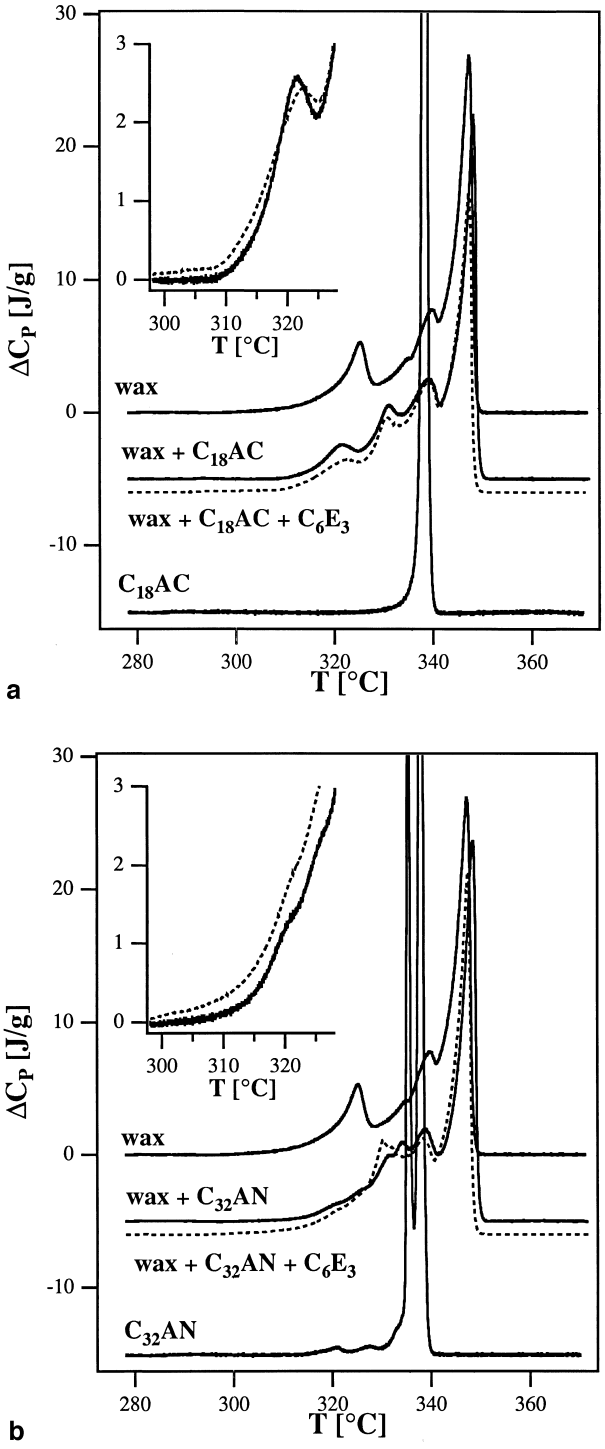

Fig. 6 **a** Calorimetric excess heat capacity profiles of barley wax (*top*), barley wax +5% $C_{18}AC$ (*centre, solid*), barley wax +5% $C_{18}AC$ + 1% C_6E_3 (*centre, dashed*) and the pure perdeuterated $C_{18}AC$ label (*bottom*). **b** Calorimetric excess heat capacity profiles of barley wax (*top*), barley wax +5% $C_{32}AN$ (*centre, solid*), barley wax +5% $C_{32}AN$ + 1% C_6E_3 (*centre, dashed*) and the pure perdeuterated $C_{32}AN$ label (*bottom*)

In all experiments, however, the addition of labels only has a minor effect on the transition point of the highest melting component which most likely reflects the C_{26}-alcohol melting (see discussion). Also, the surfactant has only a minor (but measurable) effect on the C_p-traces. More importantly, the major calorimetric events take place at temperatures above the apparent melting point in NMR. In all calorimetric experiments the melting enthalpy was constant within experimental error (200±5 J/g). It should be noted at this point that visual observation of the macroscopic appearance of the wax as a function of temperature (in a water bath) detected a softening of the sample at temperatures above 333 K and a melting at 348 K, in agreement with the most pronounced calorimetric event. No melting was obvious at 318 K.

3.3 Diffusion experiments

Desorption kinetics of the ^{14}C-labelled compounds C_{18}AC and C_{32}AN in recrystallized barley wax were successfully linearized if the relative amount desorbed (M_t/M_0) was plotted versus the square root of time and D could be calculated from the slope of the regression lines fitted to the linear portion of the linearized desorption kinetics (Figs. 7 and 8). With C_{18}AC D was identical and completely independent of the mode of loading (internal versus external) of the wax samples (Fig. 7). With C_{32}AN, however, D was strongly dependent on the mode of loading the wax samples since D was a factor of about 2400 higher when the radiolabelled alkane was applied to the wax from an external donor solution compared to the addition of the radiolabelled alkane to the wax/chloroform solution prior to its recrystallization (Fig. 8).

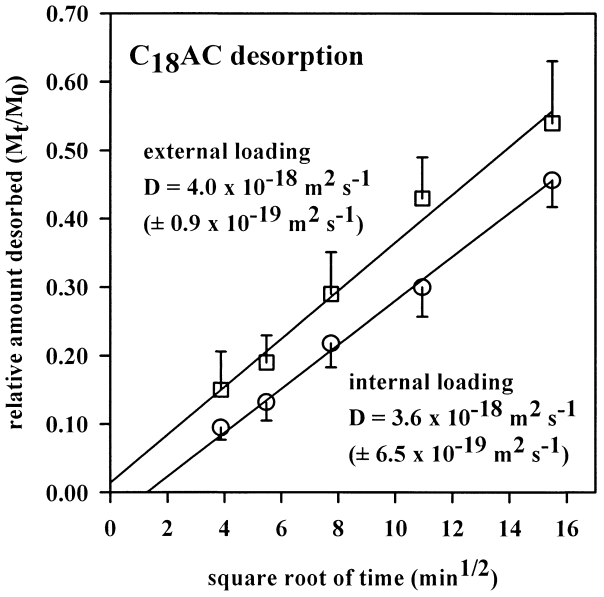

Fig. 7 Linearized desorption kinetics of octadecanoic acid (C_{18}AC) from barley wax after internal and external loading of the wax. Values of D are given as means of five repetitions with 95% confidence intervals

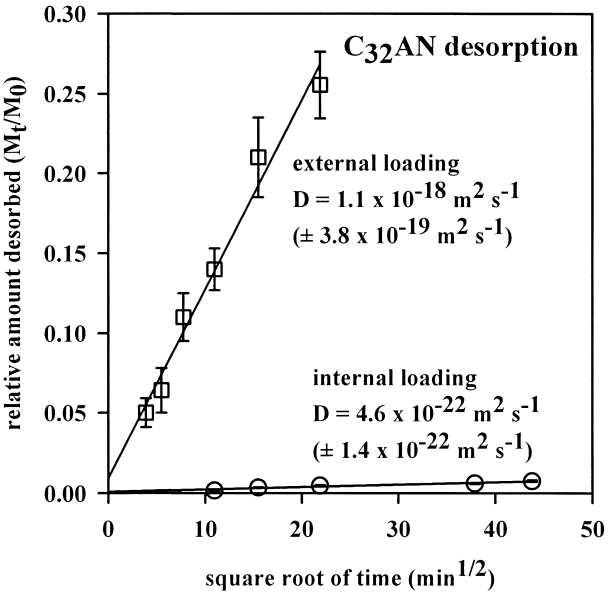

Fig. 8 Linearized desorption kinetics of dotriacontane (C_{32}AN) from barley wax after internal and external loading of the wax. Values of D are given as means of five repetitions with 95% confidence intervals

4 Discussion

4.1 ^{2}H-NMR and calorimetric experiments

The most striking finding of this work is the apparent difference in the melting points in ^{2}H-NMR and in calorimetry. We found that for the two different labels the spectra became completely isotropic at 313 K for the C_{18}AC and at 318 K for the C_{32}AN label, respectively. Solid state ^{2}H-NMR in the past has been frequently used to monitor the melting of pure alkanes (Taylor et al. 1983) and especially of lipids in membranes (for reviews see Seelig 1977; Seelig and Seelig 1980; Mantsch et al. 1977; Smith 1983). The chemical shift anisotropy leads to broad, structured spectra of solids, reflecting the random orientations of the deuterated molecules in a non-oriented solid. Owing to quadrupolar splitting the spectra are symmetric towards their origin. Upon fast rotation this spectral anisotropy is averaged into a single spectral line. Thus the spectral shape is an indicator of the fluidity and the motional degree of freedom of the spin labels. The typical correlation time that leads to motional narrowing is of the order of 10^{-5} seconds (Smith 1983). Therefore, an isotropic spectral line is evidence for a rotational correlation time of the labels much faster than 10 microseconds.

However, an isotropic spectral component is not necessarily indicative of the melting of the complete matrix. As shown by Smith and Ekiel (1984), in an aqueous environment lipid vesicles smaller than 1000 Å lead to isotropic spectra in phosphorus NMR, which has a time sensitivity comparable to ^{2}H-NMR. Thus, solid particles of small size in a fluid environment also display isotropic spectra. Some

motional averaging takes place even at the molecular level as has previously been shown in electron spin resonance (ESR)-experiments which yield a spectral narrowing at about 318 K, consistent with the NMR-measurements presented here (Schreiber et al. 1996 b). However, the sensitive time scale of ESR is much smaller (in the nanosecond regime) and it is therefore more sensitive to single molecular motion.

The disappearance of the rigid spectral component in Figs. 2 and 4 at about 318 K is evidence for the fast rotational movement of the labels. As already mentioned, this finding is consistent with both a rotational movement of the single labels and the movement of solid particles significantly smaller than 1000 Å in diameter. Calorimetry provides information both on thermotropic events and on the mixing behaviour of molecules (Lee 1977; Heimburg and Marsh 1992). Figure 6 a, b indicate that the major calorimetric events take place above 318 K and that the NMR-labels display miscibility with a heterogeneous wax matrix.

This leads to the following conclusions: The change in fluidity, monitored in NMR, does not lead to a significant absorption of heat and therefore does not correspond to a co-operative melting of a wax component as in a crystalline matrix. Thus, a non-cooperative melting of a minor fraction of the wax must be responsible for the increase in fluidity, indicating the presence of an amorphous or glassy matrix in the wax. This is supported by the presence of an isotropic ^{2}H-NMR component even at temperatures below 313 K (Figs. 2 and 4). As shown in Figs. 6 a and b the addition of the label leads to changes in the melting profiles in the range 318 – 349 K. Therefore at least some components of the wax that contain labelled molecules are definitely not molten at 318 K. However, the onset of calorimetric events is at slightly lower temperatures of about 308 – 313 K, where the spectroscopic transition occurs. One has to conclude, therefore, that the labels are embedded in solid particles of small size in a fluid environment, leading to motional narrowing of the spectra without resulting in the melting of major amounts of the wax.

A further finding is the constant transition temperature of the highest temperature peak. This temperature is equal to the melting temperature of the C_{26}-alcohol, which makes up about 80% of the matrix. Recent crystallographic results by Reynhardt and Riederer (1994) demonstrate the presence of a highly ordered crystal in barley wax yielding sharp X-ray reflections peaks. Combined with the calorimetric data one may conclude that a major fraction of the C_{26}-alcohol forms a crystalline host matrix which does not contain other molecules. This matrix seems to be responsible for the overall structure of the wax and leads to a solid appearance of the wax up to 348 K (see results). Within vacancies in this matrix all the other molecular components can be found, which contain both, co-operatively melting regions and amorphous regimes, melting at lower temperatures. All NMR-labels are found in these compartments which therefore do not see any changes in the host matrix. The water permeability and transport properties of the barley wax seem to be associated with these regimes (Riederer and Schreiber 1995). The surfactant C_6E_3 does not lead to a major change in the calorimetric profiles and therefore it is likely that it affects an amorphous region of the wax which is not seen in the calorimetric experiments. Furthermore, the surfactant affects the spectra of the octadecanoic acid to yield a lower order parameter (Fig. 3) by the second moment of the spectra.

4.2 Diffusion experiments

The investigation of isolated cuticular wax samples by ^{2}H-NMR spectroscopy offers the possibility to obtain direct insight into the molecular architetcture of the wax and it must be concluded that the hypothetical wax model, postulating an amorphous and a crystalline wax phase (Riederer and Schreiber 1995), is strongly supported by the findings of this investigation. In a recent study relating the mobility of molecules varying in size and polarity in the cuticular wax of spruce (*Picea abies* (L.) Karst) and beech (*Fagus sylvatica* L.) it was found that aliphatic molecules carrying functional groups (e. g. alcoholic or carboxylic groups) always had diffusion coefficients one order of magnitude higher compared to pure alkanes of similar size (Schreiber et al. 1996 b). Since the experiments were carried out by recrystallizing the ^{14}C-labelled molecules together with the wax (internal loading of the wax) it was concluded in accordance with the wax model that the alkanes were more efficiently trapped within separate crystalline wax domains and thus exhibited significantly lower diffusion coefficients compared to alcohols and acids of similar molecular size but significantly higher polarity.

The ^{2}H-NMR experiments corroborate this interpretation since they show directly that the smaller and more polar fatty acid C_{18}AC is located in a different wax environment of lower order (Fig. 3) compared to the pure alkane C_{32}AN (Fig. 5). The difference in diffusion coefficients of C_{32}AN after internal versus external loading (Fig. 8) can only be explained if it is assumed that the C_{32}AN is located in two different phases of the wax. Recrystallization of the pure alkane together with the wax leads to an inclusion of the alkane into a more crystalline wax phase. Alternatively, from an external donor solution C_{32}AN has access solely to an amorphous wax phase, thus yielding (by orders of magnitude) higher diffusion coefficients in the wax (Fig. 8). Owing to its bulky and polar head group C_{18}AC is seems to be located in the amorphous wax phase, irrespective of the mode of loading and consequently diffusion coefficients of C_{18}AC are similar after internal and external loading of the wax (Fig. 7). However, it must be emphasised that both labels are not located in the crystalline host matrix built by the C_{26}-alcohol melting at 348 K, but forming separate domains of different degrees of order within the amorphous wax phase.

Furthermore, with C_{18}AC a significant effect of the surfactant C_6E_3 was detected by ^{2}H-NMR (Fig. 3), indicating that the polar surfactant has access to exactly that wax domain, where the more polar C_{18}AC is located. Since no effects of C_6E_3 on C_{32}AN could be observed (Fig. 5) it must

be concluded that the unpolar C_{32}AN forms a separate phase, where C_6E_3 does not have access. In accordance with the ^{2}H-NMR experiments this observation indicates again that barley wax consists of different domains of different degrees of order on a molecular scale. Different compounds such as acids, alcohols and alkanes are located in different wax fractions.

In recent years there has been some discussion about the relevance of domain connectivity in lipid bilayers (Almeida et al. 1993; Thompson et al. 1995; Vaz et al. 1989, 1990). Fluorescence recovery after photobleaching (FRAP) experiments were performed to study diffusion in mixed lipid systems. Depending on lipid composition and temperature, conditions were found where the fluorescence recovery was not complete indicating an inhibition of diffusion. This was interpreted in terms of domain connectivity of the percolation properties. A percolating cluster is a domain of complex shape within a host matrix, where it is possible to find a continuous path from one end of the sample to the other. This means that any particle restricted to the precolating domain can still diffuse through the whole sample. This is an important concept for reaction kinetics and transport properties.

A percolating domain in the barley wax would allow for the transport of water and small molecules from the inner side of the leaf to the exterior and vice versa. Isolated clusters, however, are not connected and molecules are trapped in local domains of finite size. Therefore, diffusion is inhibited. The diffusion properties of barley wax, as described above, are consistent with a situation where C_{18}AC is located in an amorphous percolating domain, whereas the C_{32}AN is found within isolated amorphous domains. Figure 9 gives a tentative schematical drawing of the barley wax architecture after recrystallization from the melt, which is consistent with the NMR, calorimetric and diffusion experiments described above. Micro-crystals containing C_{18}AC or C_{32}AN are assumed to be located within amorphous domains which are connected or isolated, respectively. The percolating amorphous cluster spans a rigid C_{26}-alcohol phase. Thus, diffusion properties are expected to be different for the two label components.

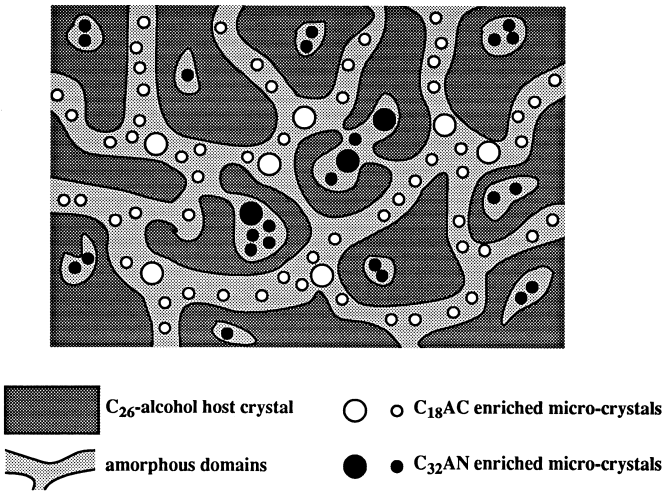

Fig. 9 Tentative schematic drawing of the molecular architecture of *Hordeum vulgare* L. (barley) leaf wax, after recrystallization from the melt, summarizing the experimental results. Embedded within a crystalline C_{26}-alcohol host matrix an amorphous, percolating domain is found, containing micro-crystals enriched in C_{18}AC. Also present are isolated amorphous domains containing C_{32}AN microcrystals. The amorphous material has a broad melting range and is supposedly fluid at 318 K. The C_{26}-alcohol host matrix melts at 348 K

4.3 Biological relevance

Plants growing in completely different habitats must be adapted on the level of their cuticular permeability to the climatic conditions dominating in these habitats. Since cuticular waxes are responsible for barrier properties of the intact cuticle it is necessary to investigate the transport properties of the waxes in order to understand and analyse the significance of the cuticular transport barrier for the whole plant. By means of ^{2}H-NMR spectroscopy of cuticular waxes isolated from plants growing naturally in habitats with different climatic conditions, it should be possible to estimate and compare the relative fluidity of the waxes. Thus, it will be possible to elucidate the ecologically relevant mechanisms of different cuticular permeabilities on a molecular level.

Furthermore, there is an important applied aspect related to the investigation of cuticular transport properties. The efficiency of many agrochemicals sprayed on leaf surfaces depends on their ability to penetrate the cuticular transport barrier successfully in order to reach their final targets in the leaf anterior. Many investigations have demonstrated that this penetration of organic molecules such as pesticides can be enhanced significantly by surfactants acting as plasticizers on the waxy transport barrier of the cuticle (Schönherr 1993 a, b; Schreiber 1995). However, up to now the exact site of action of these plasticizers in the wax has not been identified and the mechanisms of action have not been completely understood. By means of ^{2}H-NMR spectroscopy it seems possible to answer these questions and this will form the basis for an improved and more rational formulation of pesticides in the future.

Acknowledgements The authors are indebted to Dr. D. Marsh (Max-Planck-Institut für Biophysikalische Chemie, Abteilung Spektroskopie, Göttingen, Germany) for offering us the possibility to carry out this study in his laboratory. This investigation was supported by the SFB 251 (Ökologie, Physiologie und Biochemie pflanzlicher und tierischer Leistungen unter Stress) of the Deutsche Forschungsgemeinschaft.

References

Almeida PFF, Vaz WLC, Thompson TE (1993) Percolation and diffusion in three-component lipid bilayers: effect of cholesterol on an equimolar mixture of two phosphatidylcholines. Biophys J 64: 399 – 412

Baker EA (1982) Chemistry and morphology of plant epicuticular waxes. In: Cutler DF, Alvin KL, Price CE (eds) The plant cuticle. Academic Press, London, pp 139–165

Basson I, Reynhardt EC (1988) An investigation of the structures and molecular dynamics of natural waxes: II. Carnauba wax. J Phys D Appl Phys 21: 1429–1433

Bukovac MJ (1976) Herbicide entry into plants. In: Audus (ed) Herbicides, physiology, biochemistry, ecology, Academic Press, New York, pp 335–364

Büscher KE (1960) Messung der Dichte, des spezifischen Volumens und des kubischen Ausdehnungskoeffizienten plastischer Massen mit Hilfe des Haake-Konsistometers. Erdöl Kohle 13: 102–106

Cutler DF, Alvin KL, Price CE (1982) The plant cuticle. Academic Press, London

Felder RM, Huvard GS (1980) Polymers: physical properties. In: Marton L, Marton C (eds) Methods of experimental physics, vol 16, Part C. Academic Press, New York, pp 343–346

Heimburg T, Würz U, Marsh D (1992) Binary phase diagram of hydrated dimyristoylglycerol-dimyristoylphosphatidylcholine mixtures. Biophys J 63: 1369–1378

Holloway PJ (1982) Structure and histochemistry of plant cuticular membranes. In: Cutler DF, Alvin KL, Price CE (eds) The plant cuticle. Academic Press, London, pp 45–85

Kollatukudy PE (1980) Biopolyesters of plants: cutin and suberin. Science 208: 990–1000

Lee AG (1977) Lipid phase transitions and phase diagrams II. Mixtures involving lipids. Biochim Biophys Acta 472: 285–344

Mantsch HH, Saitô H, Smith ICP (1977) Deuterium magnetic resonance, applications in chemistry, physics and biology. Progr Nucl Magn Res Spectros 11: 211–258

Martin JT, Juniper BE (1970) The cuticles of plants. Edward Arnold, London

Rance M, Jeffrey KR, Tulloch AP, Butler KW, Smith ICP (1980) Orientational order of unsaturated lipids in the membranes of archeplasma laidlawii as observed by ^{2}H-NMR. Biochim Biophys Acta 600: 245–262

Reynhardt EC, Riederer M (1991) Structure and molecular dynamics of the cuticular wax from leaves of *Citrus aurantium* L. J Phys D Appl Phys 24: 478–486

Reynhardt EC, Riederer M (1994) Structure and molecular dynamics of plant waxes. II. Cuticular waxes from leaves of *Fagus sylvatica* L. and *Hordeum vulgare* L. Eur Biophys J 23: 59–70

Riederer M, Schönherr J (1985) Accumulation and transport of (2,4-dichlorphenoxy)acetic acid in plant cuticles: II. Permeability of the cuticular membrane. Ecotoxicol Environ Safety 9: 196–208

Riederer M, Schreiber L (1995) Waxes: The transport barriers of plant cutciles. In: Hamilton RJ (ed) Waxes: chemistry, molecular biology and functions. The Oily Press, West Ferry, pp 131–156

Schönherr J (1976) Water permeability of isolated cuticular membranes: The effect of cuticular waxes on diffusion of water. Planta 131: 159–164

Schönherr J (1982) Resistance of plant surfaces to water loss: transport properties of cutin, suberin and associated lipids. In: Lange OL, Nobel PS, Osmond CB, Ziegler H (eds) Encyclopedia of plant physiology, New series vol. 12 B: Physiological plant ecology, Part 2. Springer, Berlin Heidelberg New York, pp 135–179

Schönherr J (1993 a) Effects of monodisperse alcohol ethoxylates on mobility of 2,4-D in isolated plant cuticles. Pestic Sci 38: 155–164

Schönherr J (1993 b) Effects of alcohols, glycols and monodisperse ethoxylated alcohols on mobility of 2,4-D in isolated plant cuticles. Pestic Sci 39: 213–223

Schönherr J, Baur P (1994) Modelling penetration of plant cuticles by crop protection agents and effects of adjuvants on their rates of penetration. Pestic Sci 42: 185–208

Schönherr J, Riederer M (1989) Foliar penetration and accumulation of organic chemicals in plant cuticles. Rev Environ Cont Toxicol 108: 1–70

Schreiber L, Schönherr J (1993) Mobilities of organic compounds in reconstituted wax of barley leaves: determination of diffusion coefficients. Pestic Sci 38: 353–361

Schreiber L (1995) A mechanistic approach towards surfactant/wax interactions: Effects of octaethyleneglycolmonododecylether on sorption and diffusion of organic chemicals in reconstituted cuticular wax of barley leaves. Pestic Sci 45: 1–11

Schreiber L, Kirsch T, Riederer M (1996 a) Transport properties of cuticular waxes of *Fagus sylvatica* L. and *Picea abies* (L.) Karst: estimation of size selectivity and tortuosity from diffusion coefficients of aliphatic molecules. Planta 197: 104–109

Schreiber L, Riederer M, Schorn K (1996 b) Mobilities of organic compounds in reconstituted cuticular wax of barley leaves: effects of monodisperse alcoholethoxylates on diffusion of pentachlorophenol and tetracosanoic acid. Pestic Sci (in press)

Seelig J (1977) Deuterium magnetic resonance: theory and application to lipid membranes. Quart Rev Biophys 10: 353–418

Seelig J, Seelig A (1980) Lipid conformation in model membranes and biological membranes. Quart Rev Biophys 13: 19–61

Sitte P, Rennier R (1963) Untersuchungen an cuticularen Zellwandschichten. Planta 60: 18–40

Smith ICP (1983) Deuterium NMR. In: Laszlo P (ed) NMR of Newly Accessible Nuclei, vol 2. Academic Press, New York, pp 1–26

Smith ICP, Ekiel IH (1984) Phosphorus-31 NMR of phospholipids in membranes. In: Gorenstein DG (ed) Phosphorus-31 NMR – Principles and applications. Academic Press, New York, pp 447–475

Taylor MG, Kelusky EC, Smith CP, Casal HL, Cameron DG (1983) A ^{2}H NMR study of the solid-phase behavior of nonadecane. J Chem Phys 78: 5108–5112

Thompson TE, Sankaram MB, Biltonen RL, Marsh D, Vaz WLC (1995) Effects of domain structure on in-plane reactions and interactions. Mol Memb Biol 12: 157–162

Vaz WLC, Melo ECC, Thompson TE (1989) Translational diffusion and fluid domain connectivity in a two-compartment, two-phase phospholipid bilayer. Biophys J 56: 869–876

Vaz WLC, Melo ECC, Thompson TE (1990) Fluid-phase connectivity in an isomorphous, two-compartment, two-phase phosphatidylcholine bilayer. Biophys J 58: 273–275

Walton TJ (1990) Waxes, cutin and suberin. Meth Plant Biochem 4: 105–158